A Method of Moments Model for VHF Propagation

Joel T. Johnson, *Member, IEEE*, Robert T. Shin, *Senior Member, IEEE*, John C. Eidson, *Member, IEEE*, Leung Tsang, *Fellow, IEEE*, and Jin Au Kong, *Fellow, IEEE*

***Abstract*— Predictions of a numerical model for site specific very high frequency (VHF) propagation over irregular terrain are compared to experimental data and to other propagation models. The numerical model is based on an iterative version of the method of moments (MOM) known as the banded matrix flat surface iterative approach (BMFSIA) for either perfectly conducting or penetrable surfaces rough in one direction only. Due to the large size of the numerical problem (65 000 to 130 000 unknowns), a parallel implementation of the method is presented and applied in the simulations. Comparisons with measurement data show good agreement overall and also illustrate the sensitivity of the model to input terrain profiles. Comparisons with other propagation models show good agreement also in cases where these models are expected to be valid and further clarify the limitations of the approximations made in these methods.**

***Index Terms*—Numerical methods, radio propagation.**

I. Introduction

SITE-specific very high frequency (VHF) propagation models remain a subject of continuing interest. A number of approximate methods exist and have been applied successfully in specific cases, but the limitations of the approximations of these models remain unclear. One such model, known as spherical earth with knife edges (SEKE) [1], uses a weighted average of analytic solutions for the multipath, spherical earth, and knife-edge diffraction contributions which depends on the transmitter, receiver, and terrain geometries. Although SEKE has been shown to have good general agreement with experimental data, clarification of discrepancies is difficult given uncertainties both in the underlying electromagnetic approximations and in the input terrain profiles. Another approach which has been studied extensively involves the use of the parabolic approximation to the Helmholtz equation [2]–[8]. Methods based on the parabolic wave equation (PWE) neglect the contribution of backscattered fields which can become significant when obstacles are near the transmitter [9]. Again, comparisons with measurement data show good general agreement but differences that exist are difficult to explain.

Numerically exact methods have also been investigated for small obstacles [9], [10], but the large electromagnetic distances involved in more general propagation problems makes numerical methods impractical. Given that at 150 MHz, one kilometer of terrain corresponds to 500λ, and that typical VHF propagation problems involve distances in the tens of kilometers, a numerical model needs to be able to solve problems with profiles on the order of tens of thousands of wavelengths long. Such electromagnetic distances are usually considered too large for numerical methods. A numerically exact model is desirable because it avoids any approximations in the solution and can, therefore, be used to validate other nonexact methods and to demonstrate conclusively the sensitivity of the true solution to input terrain parameters.

In this paper, a numerically exact model based on the recently developed banded matrix iterative approach (BMIA) [11]–[14] to the method of moments (MOM) is presented which enables the solution of practical propagation problems. Although this model remains computationally complex, the iterative method used results in greater efficiency in the MOM solution, so that predictions can be generated from a single DEC AXP 300 workstation in approximately two CPU days for a ten thousand wavelength problem. Section II describes the basic propagation configuration and the formulation of the MOM solution. The method is then validated in Section III through comparison with exact solutions for some simple geometries, and a parallel implementation which allows the solution of larger problems in reasonable amounts of time is discussed in Section IV. A comparison of model predictions with experimental data in Section V shows overall agreement between the model and measurements to be good, and demonstrates the sensitivity of terrain-based propagation models to input terrain parameters. Section VI compares these predictions with the SEKE and PWE methods, and Section VII presents final conclusions.

II. Formulation and Numerical Method

A typical VHF propagation problem involves predicting the power measured by a receiver as a function of altitude at a given distance away from a like polarized transmitter and

Manuscript received September 23, 1995; revised March 14, 1996. This work was supported by ONR contract N00014-92-J-4098, NASA contract 958461, the Joint Services Electronics Program under contract DAAH04-95-1-0038, a National Science Foundation graduate fellowship, and the Department of the Air Force, contract F19628-95-C-0002.

J. T. Johnson is with the Department of Electrical Engineering and ElectroScience Laboratory, The Ohio State University, Columbus, OH 43210 USA.

R. T. Shin and J. Eidson are with the Lincoln Laboratory, Massachusetts Institute of Technology, Lexington, MA 02173 USA.

L. Tsang is with Electromagnetics and Remote Sensing Laboratory, Department of Electrical Engineering, University of Washington, Seattle, WA 98195 USA.

J. A. Kong is with the Department of Electrical Engineering and Research Laboratory of Electronics, Massachusetts Institute of Technology, Cambridge, MA 02139 USA.

Publisher Item Identifier S 0018-926X(97)00448-1.

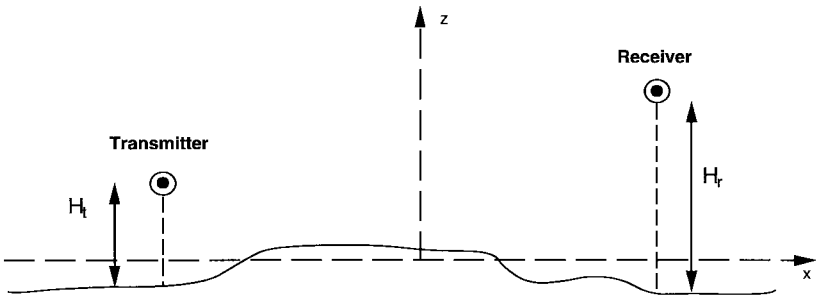

Fig. 1. Geometry of propagation problem.

above an irregular terrain profile, as shown in Fig. 1. When distances separating the transmitter and receiver are very large and the terrain is not rapidly varying on an electromagnetic scale, a Fresnel zone argument can be applied which illustrates that terrain outside of the plane of incidence has little effect so that a two-dimensional model is sufficient to capture the physics of the problem. Thus, the MOM formulation will assume a surface profile which is irregular only in the plane of incidence (taken to be the x–z plane) and constant perpendicular to the plane of incidence (the y direction).

For in-plane incidence in a two-dimensional problem, Maxwell's equations decouple into dual equations for TE and TM waves, and a scalar Kirchhoff diffraction integral in terms of E_y for the TE case and H_y for the TM case can be applied using the two-dimensional Hankel function form of the Green's function [15]. Equations for a dielectric surface medium are

$$\frac{E_y(\overline{r})}{2} = E_y^{inc} + \int dS' \cdot \left\{ E_y(\overline{r}') \frac{\partial g(\overline{r},\overline{r}')}{\partial n} - g(\overline{r},\overline{r}') \frac{\partial E_y(\overline{r}')}{\partial n} \right\} \tag{1}$$

$$\frac{E_y(\overline{r})}{2} = -\int dS' \cdot \left\{ E_y(\overline{r}') \frac{\partial g_1(\overline{r},\overline{r}')}{\partial n} - g_1(\overline{r},\overline{r}') \left(\frac{\partial E_y(\overline{r}')}{\partial n} \right)_1 \right\} \tag{2}$$

for the TE case with incident field E_y^{inc} and

$$\frac{H_y(\overline{r})}{2} = H_y^{inc} + \int dS' \cdot \left\{ H_y(\overline{r}') \frac{\partial g(\overline{r},\overline{r}')}{\partial n} - g(\overline{r},\overline{r}') \frac{\partial H_y(\overline{r}')}{\partial n} \right\} \tag{3}$$

$$\frac{H_y(\overline{r})}{2} = -\int dS' \cdot \left\{ H_y(\overline{r}') \frac{\partial g_1(\overline{r},\overline{r}')}{\partial n} - g_1(\overline{r},\overline{r}') \left[\frac{\partial H_y(\overline{r}')}{\partial n} \right]_1 \right\} \tag{4}$$

for the TM case with incident field H_y^{inc} where the domain of integration is the surface profile S' in the plane of incidence and a principal value integration is implied. Note that the above formulation neglects any propagation effects due to atmospheric refraction so that only the standard linear refractive-index approximation is possible to model these effects through use of an earth radius modification. Such an approach will be used when comparing with propagation measurements in Section V. Continuity of tangential field components E_y and H_y is implicit in the above formulations with continuity of the along profile field component yielding

$$\frac{\partial E_y(\overline{r}')}{\partial n} = \alpha \left[\frac{\partial E_y(\overline{r}')}{\partial n} \right]_1 \tag{5}$$

$$\frac{\partial H_y(\overline{r}')}{\partial n} = \beta \left[\frac{\partial H_y(\overline{r}')}{\partial n} \right]_1 \tag{6}$$

where $\alpha = 1$ for the TE case (nonmagnetic medium) and $\beta = \epsilon_1/\epsilon_2$ for TM and in-plane incidence is assumed [16]. Also, in the above equation

$$g_j(\overline{r},\overline{r}') = \frac{i}{4} H_0^{(1)}(k_j|\overline{r} - \overline{r}'|) \tag{7}$$

where $k_j = \omega\sqrt{\mu_0 \epsilon_j}$ is the propagation constant in medium j.

The above formulation gives two integral equations in two unknowns (E_y and $\partial E_y/\partial n$ or H_y and $\partial H_y/\partial n$) on the surface profile. Applying a point-matching MOM technique [17] results in a matrix equation in terms of the unknown pulse-basis function expansion coefficients of these fields which can be written as

$$\overline{\overline{Z}}\,\overline{I} = \overline{V} \tag{8}$$

where $\overline{I}$ is a vector containing the expansion coefficients, and $\overline{V}$ contains the incident field evaluated at points on the surface profile. Elements of the impedance matrix $\overline{\overline{Z}}$ are proportional to Hankel functions of order zero or order one evaluated at arguments corresponding to distances between individual points on the surface profile. Tables of the zero- and first-order Hankel functions are stored in the computer code implemented to avoid multiple calls to Hankel routines.

In the BMIA of reference [11], the above matrix equation is solved iteratively by expressing the matrix $\overline{\overline{Z}}$ as the sum of a strong matrix $\overline{\overline{Z}}^{(s)}$ which contains the elements of $\overline{\overline{Z}}$ to within a specified bandwidth from the diagonal, and a weak matrix $\overline{\overline{Z}}^{(w)}$ which contains the remaining elements. The weak matrix contribution is included iteratively so that the solution is obtained by solving

$$\overline{\overline{Z}}^{(s)}\overline{I}^{(1)} = \overline{V} \tag{9}$$

initially, and then iterating

$$\overline{\overline{Z}}^{(s)}\overline{I}^{(n+1)} = \overline{V} - \overline{\overline{Z}}^{(w)}\overline{I}^{(n)} \tag{10}$$

until convergence is observed in $\overline{I}^{(n)}$. The BMIA requires solution of the banded matrix equation on each iteration and then a weak matrix multiply so that the overall method is $O(N^2)$ for an $N \times N$ matrix, but convergence is typically faster than other $O(N^2)$ methods. Direct solution of the banded matrix equation is practical when enough memory resources are available to store the banded matrix. However, in the case of propagation problems, even storage of the banded matrix is impossible if a reasonable bandwidth is desired in the computations. Also, relatively large bandwidths are required in the BMIA due to the fact that weak terms are neglected entirely in the banded matrix equation solution.

In this paper, a method similar to those applied for surfaces rough in two dimensions [13], [14] is adopted in an attempt to alleviate some of the problems associated with the BMIA. In this method—known as the banded matrix flat surface iterative approach (BMFSIA)—the original matrix $\overline{\overline{Z}}$ is decomposed into the sum of the same BMIA strong matrix $\overline{\overline{Z}}^{(s)}$, a new "flat-surface" matrix $\overline{\overline{Z}}^{(fs)}$, which contains an approximation to the terms of the BMIA weak matrix, and a new weak matrix $\overline{\overline{Z}}^{(w)}$, which contains the difference between BMIA weak matrix elements and elements of the flat-surface matrix. The flat-surface matrix approximates coupling between points on the surface by assuming that they lie at the same elevation so that matrix elements are evaluated using

$$g_j^{(fs)} = \frac{i}{4} H_0^{(1)}(k_j|x - x'|) \tag{11}$$

and

$$\frac{\partial g_j^{(fs)}}{\partial n} = 0 \tag{12}$$

instead of g_j and $\partial g_j/\partial n$ as in the BMIA weak matrix.

Again, the weak matrix contribution is included iteratively so that the solution is obtained by solving

$$[\overline{\overline{Z}}^{(s)} + \overline{\overline{Z}}^{(fs)}]\overline{I}^{(1)} = \overline{V} \tag{13}$$

initially and then iterating

$$[\overline{\overline{Z}}^{(s)} + \overline{\overline{Z}}^{(fs)}]\overline{I}^{(n+1)} = \overline{V} - \overline{\overline{Z}}^{(w)}\overline{I}^{(n)} \tag{14}$$

until convergence is observed in $\overline{I}^{(n)}$. However, in the BMFSIA another iterative method is used to solve the strong plus flat-surface matrix equation on each weak iteration, resulting in nested iterative methods analogous to those of [13]. The advantage of the "inner" iterative technique which uses a conjugate gradient solver is that inclusion of flat surface terms is not computationally expensive since flat-surface matrix multiplies can be performed using the FFT. Also, the conjugate gradient solver of the inner iteration is more easily parallelizable than a direct banded matrix solver with no storage (as will be described in Section IV).

Once the induced fields on the surface are obtained, the Kirchhoff diffraction integral can again be used to calculate the scattered field at the receiver and, therefore, the total power received. Transmitting antennas are modeled as either electric or magnetic line sources for the TE and TM cases, respectively, so that a zero-order Hankel function incident field is produced on the surface. Although a vertical electric dipole antenna does not have the same pattern as a horizontal magnetic dipole, the long distances involved in propagation problems again result in only minor effects due to differences in antenna patterns.

III. Model Validation

To validate the model, comparisons with published results and with exact solutions for some simple geometries were performed. Issues to be considered in the MOM model are the discretization level required, the effect of finite surface size on the simulations, the importance of retaining all weak iterations in the BMFSIA, and the necessity of modeling surface-medium dielectric properties.

Predicted one-way propagation factors (denoted by the symbol F^2 and defined as the ratio of the power received to that which would be received in free space) at a range of 236 wavelengths for a horizontally polarized (TE) line source above a flat perfectly conducting plane were compared with the analytical solution to assess the required sampling rate in the numerical solution. Surface currents were sampled at four points per electromagnetic wavelength, and the model was found to accurately capture the multipath interference effects of this problem with a maximum absolute error of 0.03 in the linear propagation factor. Surface currents for a TM line source above a flat impedance plane and for a TE line source in front of a perfectly conducting semicylinder were also compared with references [9] and [18], respectively, and found to be in excellent agreement. Four points per wavelength sampling was again found sufficient for the TM line-source case, but a higher sampling rate of 20 points per wavelength was required in the TE comparison due to the need to accurately sample the geometry of a 0.5λ radius semicylinder. The simple point-matching MOM used requires a high-sampling density in cases where surface structures are rapidly varying on an electromagnetic scale. However, since terrain profiles to be studied with the model are extremely undersampled on an electromagnetic scale and, therefore, very slowly varying, four points per wavelength sampling is sufficient to model the obtained field variations.

To investigate the effect of finite surface size on model predictions, simulations were run for the perfectly conducting wedge geometry of reference [19], shown in Fig. 2, at 100 MHz and TE polarization. Identical wedge geometries with differing total surface sizes L of 5 km (1666λ) and 10 km (3333λ) were created by adding additional flat-surface regions of 2.5 km on either side of the wedge for the 10-km surface. Results are shown in Fig. 3 and demonstrate that finite surface size has little effect on model predictions. Predictions for a surface size of 5 km were also compared with the geometric theory of diffraction (GTD) approach of [19] and again found to be in excellent agreement.

Since typical propagation problems involve very large distances, an initial consideration of the BMFSIA technique suggests that complete neglect of the weak matrix might be reasonable. This issue is studied in Fig. 4, where the results of Fig. 3 for a surface size of 1666λ are plotted at each weak iteration of the BMFSIA, using a bandwidth of

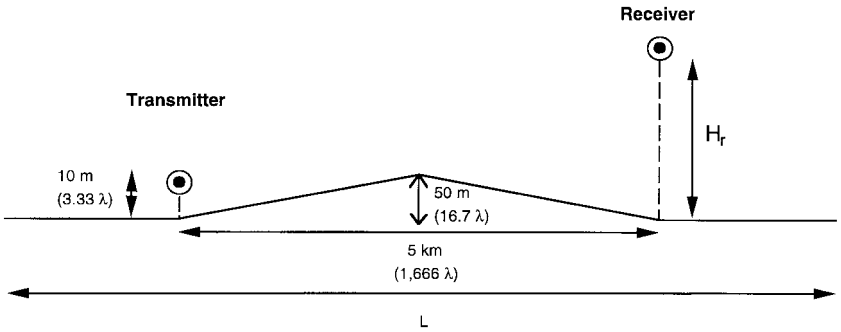

Fig. 2. Wedge geometry of [19].

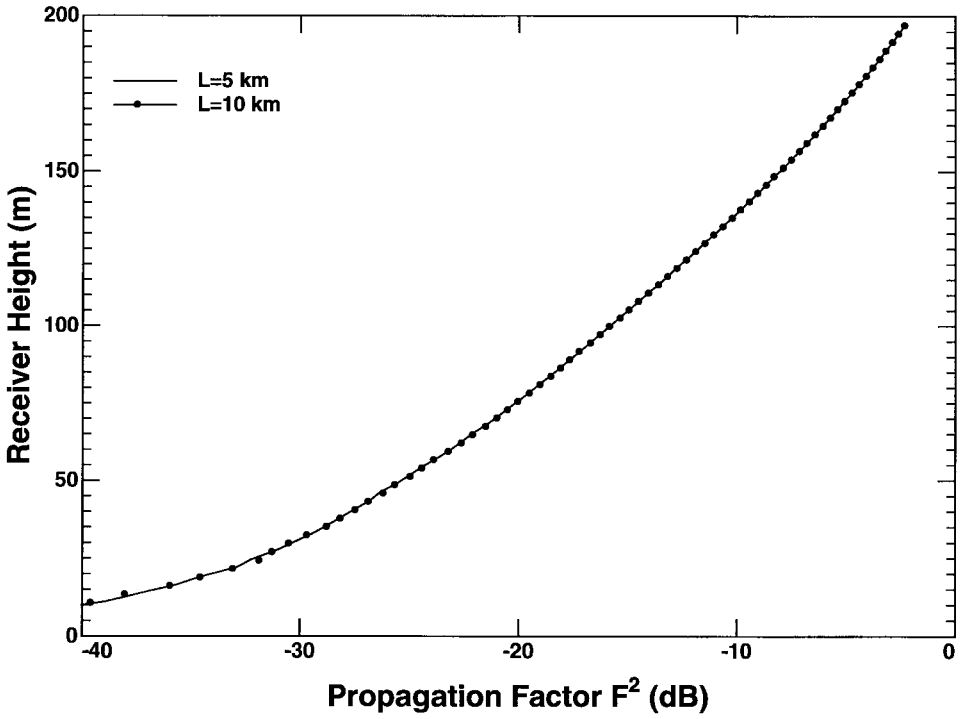

Fig. 3. Predicted one-way propagation factor for perfectly conducting wedge. TE polarization: comparison of results for varying total surface size.

1000 points or 250λ. These curves clearly demonstrate the importance of including weak matrix contributions, especially in the diffraction region, where a convergent result is not obtained until an error of less than 0.1% is reached in the BMFSIA.

A final issue in the MOM model involves the importance of modeling surface-medium dielectric properties. As discussed in [7], both TE and TM polarized model predictions usually fit well by assuming a TE polarized transmitter and a perfectly conducting surface. This is demonstrated in measurement data as well which is usually independent of polarization at low grazing angle geometries over farmland and forest and well matched by perfectly conducting surface models for farmland (but not forest) terrains. Modeling the surface as being perfectly conducting is advantageous since one of the two unknown fields on the surface vanishes and the matrix equation reduces in size by a factor of two. In addition, the need to sample surface fields on the scale of the wavelength inside the medium is eliminated. To investigate this point, simulations were run for the 1666λ wedge geometry of Fig. 2, using both perfectly conducting and penetrable media in TE and TM polarizations. A dielectric constant of $\epsilon = (6.0, 0.63)$ (a conductivity of 0.0065 S/m at 167 MHz) was assumed for the penetrable case for matrix sizes of 6664 in the perfectly conducting code, and 32 768 in the penetrable code. The additional factor of $\sqrt{6}$ in penetrable matrix size results from sampling surface field unknowns on approximately the scale of the wavelength in the surface medium.

Predicted one-way propagation factors are shown in Fig. 5 for TE and TM polarizations. The comparison shows little difference between the penetrable surface TE and TM predictions and the perfectly conducting TE prediction. The perfectly conducting TM prediction is seen to differ, as can be explained by observing that for TM polarization, the Brewster angle effect results in a reflection coefficient of $+1$ in the perfectly conducting case as one approaches grazing, but -1 in the penetrable case for angles closer to grazing than the Brewster angle. Due to similarity of the TE and TM predictions,

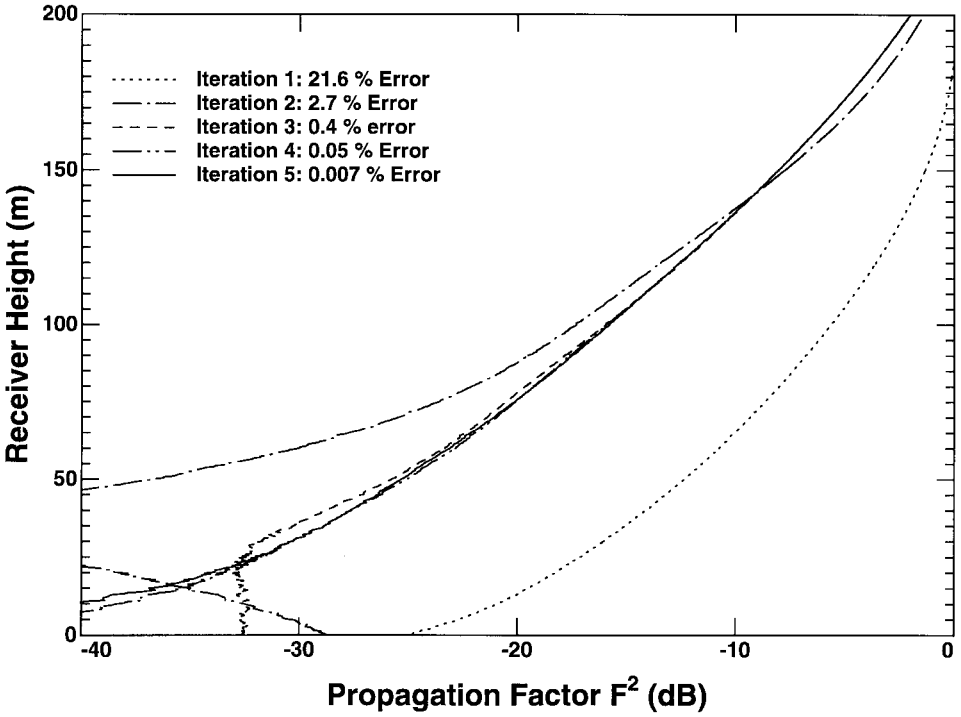

Fig. 4. Predicted one-way propagation factor for perfectly conducting wedge. TE polarization: model predictions on each BMFSIA weak iteration.

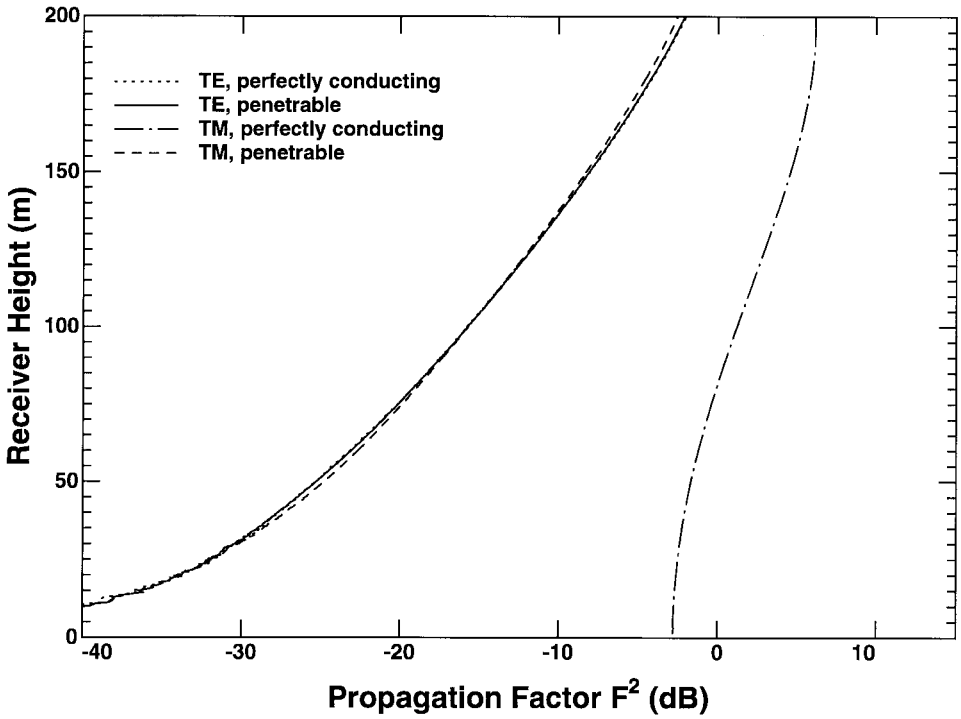

Fig. 5. Predicted one-way propagation factor for perfectly conducting wedge. TE and TM polarizations: comparison of perfectly conducting and penetrable surfaces.

simulations in the following sections were run only for TE polarization and a perfectly conducting surface profile.

IV. Parallel Implementation

One particular terrain profile of interest—Magrath NW37—which will be described in more detail in the next section, has a length of 37 km, or 20 600λ at the 167 MHz frequency where measurement data were taken. An additional 14-km buffer zone was added to the terrain profile to avoid any potential edge effects, for a total of 113 500 unknowns in the BMFSIA solution. The BMFSIA code was run for this case on a DEC AXP-300 Alpha

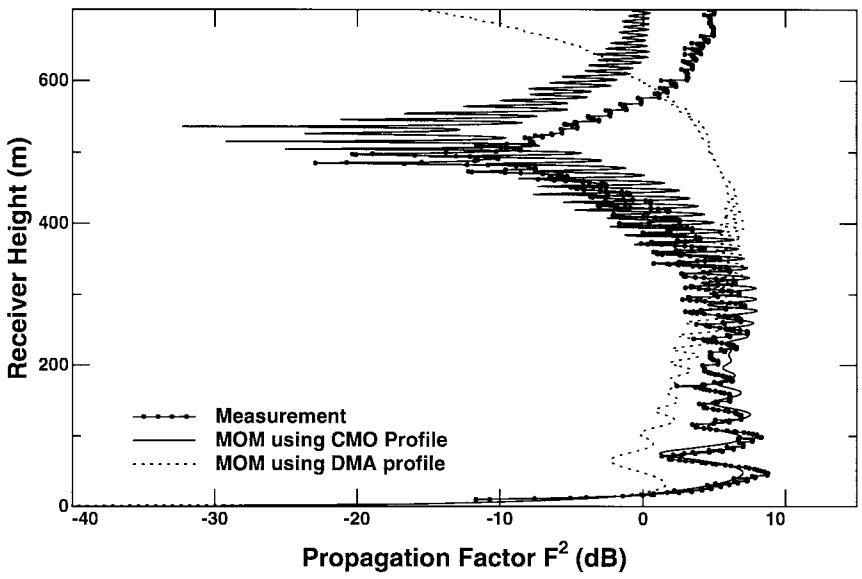

(a)

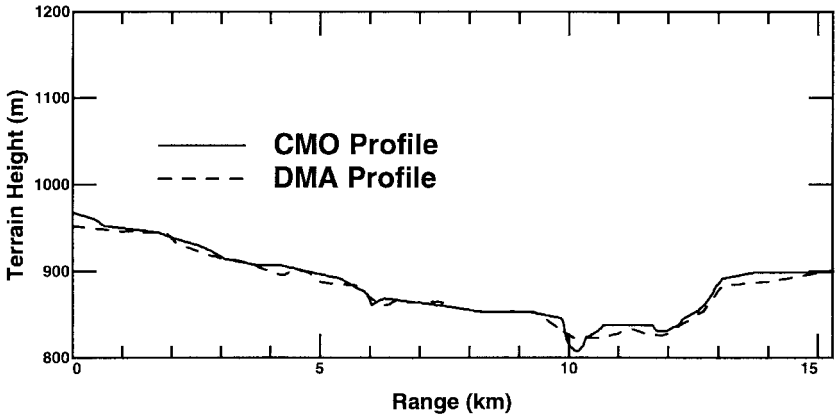

(b)

Fig. 6. Comparison of MOM predictions with measurement data. (a) One-way propagation factor. (b) Beiseker N15 terrain profiles.

workstation and was found to require approximately one week of CPU time. To reduce this large time requirement, a parallel implementation of the BMFSIA was developed and is described in this section.

Since the BMFSIA is composed of two iterative methods which both require matrix multiplies with a vector, parallelization of the code is achieved by performing these multiplies in parallel. A simple master-slave configuration is used, in which the master program broadcasts the vector to be multiplied to S slave programs which then perform the multiplication for N/S rows of the matrix. These slaves then broadcast their individual solutions back to the master program which adds up the results to obtain the matrix vector product. This code was implemented on 16 nodes of the IBM SP/2 parallel computer at the Maui High-Performance Computing Center, using the public domain Parallel Virtual Machine (PVM) code [20] as the message-passing library. Due to the large size of the problem and the need for recalculation of all matrix elements on every iteration, communication costs represent relatively little of the overall program time so that the parallelization for this code is relatively efficient. Comparison of the workstation and parallel versions showed a parallel speed-up factor of approximately 70% of the number of nodes used in the calculations.

Several additional methods were used to reduce computational time as well. A physical optics initial guess was used to begin the iterative process, and was found to reduce the number of conjugate gradient iterations required in the first-order solution. A diagonal block preconditioner was used in the conjugate gradient method, and matrix multiplies made use of the semisymmetric properties of the impedance matrix. Finally, an asymptotic expansion of the Hankel function was used in the slave program, weak-matrix multiply routines, so that storing the Hankel function table at large distances was not required.

V. Comparison with Experimental Data

A large database of propagation measurements for sites in Canada has been compiled by Lincoln Laboratory (as is described in [1]) for both TE and TM polarizations. Terrain profile data were obtained from both hand-read Canada Map Office (CMO) maps and Defense Mapping Agency (DMA)

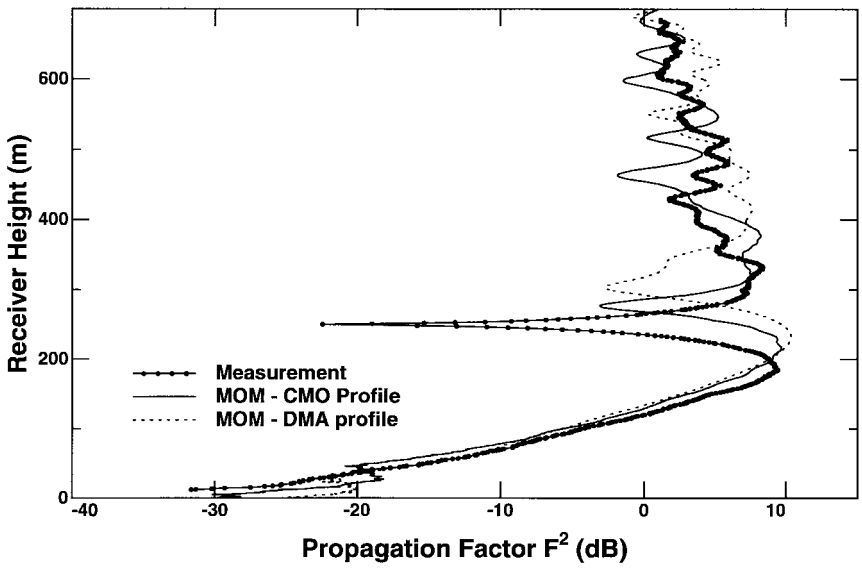

(a)

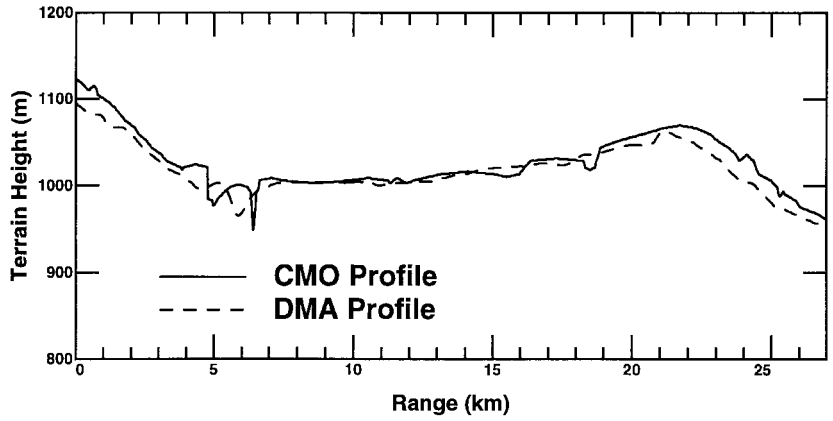

(b)

Fig. 7. Comparison of MOM predictions with measurement data. (a) One-way propagation factor. (b) Magrath NW27 terrain profiles.

digital files at horizontal resolutions of 30 and 100 m, respectively, with 1-m vertical resolution in both cases. Three locations (called Beiseker N15, Magrath NW27, and Magrath NW37, respectively) for which SEKE predictions deviated from measured data were selected for use in the MOM simulation. The terrain of these three locations was farmland with only scattered and isolated trees or buildings present so that a surface scattering model should suffice to capture the relevant ground-propagation effects. Measurements were taken at 167 MHz with a transmitting antenna height of 18.3 m above ground level, and terrain profiles were linearly interpolated between points for use in the BMFSIA solution. Atmospheric and earth curvature effects were included in the model by assuming the standard 4/3 earth radius approximation for a linear atmospheric refractive index profile so that specified terrain-elevation data were fit to a sphere of radius 4/3 times the true earth radius.

Figs. 6–8 show comparisons between model predictions and measurement data for the three locations using CMO terrain profiles. Overall agreement is observed to be very good for these cases, and the MOM model is seen to capture the multipath and diffraction contributions accurately both in the interference and shadowed regions. However, some discrepancies (particularly in the location of the first multipath null) exist which require clarification. One possible source of these differences is the accuracy of input terrain profiles. Also included in Figs 6–8 are DMA profile MOM predictions for the same three locations. Results are seen to be very sensitive to input terrain data, especially in the Beiseker N15 case (Fig. 6), where profile differences close to the transmitter location influence the specular point slope and significantly alter predictions. Predictions using the higher resolution CMO profiles are seen to be closer to measurements for all three cases. Note that fixed transmitting and receiving antenna heights above the terrain profile lead to significant differences in the absolute height above sea level for these antennas in the CMO and DMA profiles. However, since an absolute height above mean sea level at the time of the measurements was not known, the comparisons of Figs. 6–8 illustrate the differing conclusions that can be reached for a differing terrain profiles, and show that accurate terrain profile measurements are required to obtain accurate predictions of the propagation factor.

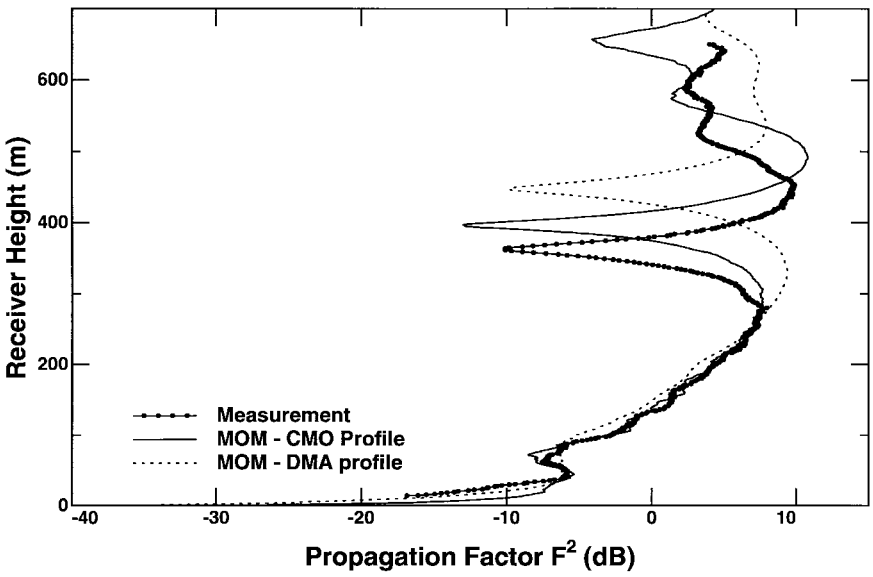

(a)

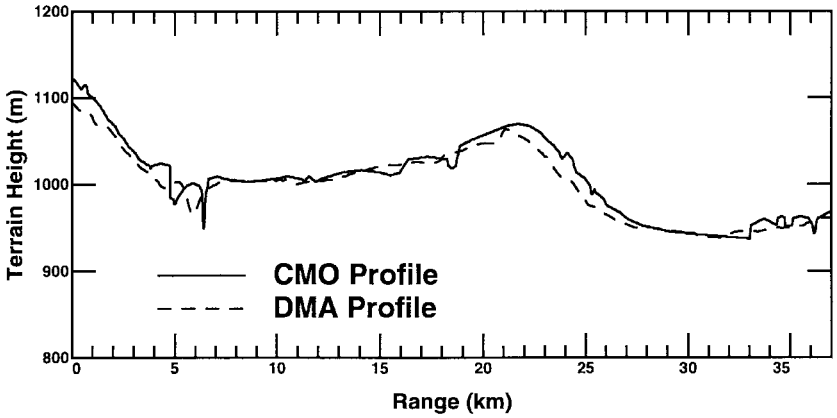

(b)

Fig. 8. Comparison of MOM predictions with measurement data. (a) One-way propagation factor. (b) Magrath NW37 terrain profiles.

A second possible source of differences between BMFSIA predictions and measurement data involves any anomalous propagation effects due to deviations in the atmospheric index of refraction from the assumed linear profile. Since no refractivity profile information is available for the measurements considered, an improvement of the BMFSIA predictions in this regard is not possible, making a complete understanding of BMFSIA/measurement differences difficult. However, statistical radiosonde profiles collected from nearby World Meterological Organization (WMO) stations indicate that anomalous propagation conditions occur in these regions only a small percentage (less than 10%) of the time [21]. Note that the next section will compare BMFSIA predictions with those of the approximate methods for identical terrain and atmospheric refractivity profiles, eliminating these uncertainties in its conclusions.

VI. Comparison with Other Propagation Models

Figs. 9–11 compare SEKE, PWE, and MOM predictions for the CMO profile of the three locations. The 1994 beta version of SEKE was used in these comparisons which is a revision of the 1986 version described in [1] with improvements to the four basic SEKE propagation loss algorithms for single and multiple specular multipath, knife-edge diffraction, and spherical earth diffraction. PWE results were generated using a split-step Fourier algorithm similar to [7] developed at Massachusetts Institute of Technology [22], and assumed a standard atmospheric profile and a Gaussian beam initial-field distribution. Terrain-profile inputs to the PWE code were smoothed with a five-point averaging filter to avoid large second derivatives, and calculations were performed for 1- and 25-m step increments in height and range, respectively. Figs. 9–11 show a good overall level of agreement between the three methods, demonstrating that the PWE and SEKE models are giving an accurate prediction for the terrain-profile input. However, some differences are observed which illustrate the limitations of the SEKE and PWE methods.

SEKE predictions become inaccurate in cases where both multipath and diffraction contributions are significant, and underestimate the strength of the first maximum above the shadowed region in particular, as shown in Figs. 10 and 11. Similar underestimations are observed for knife-edge diffrac-

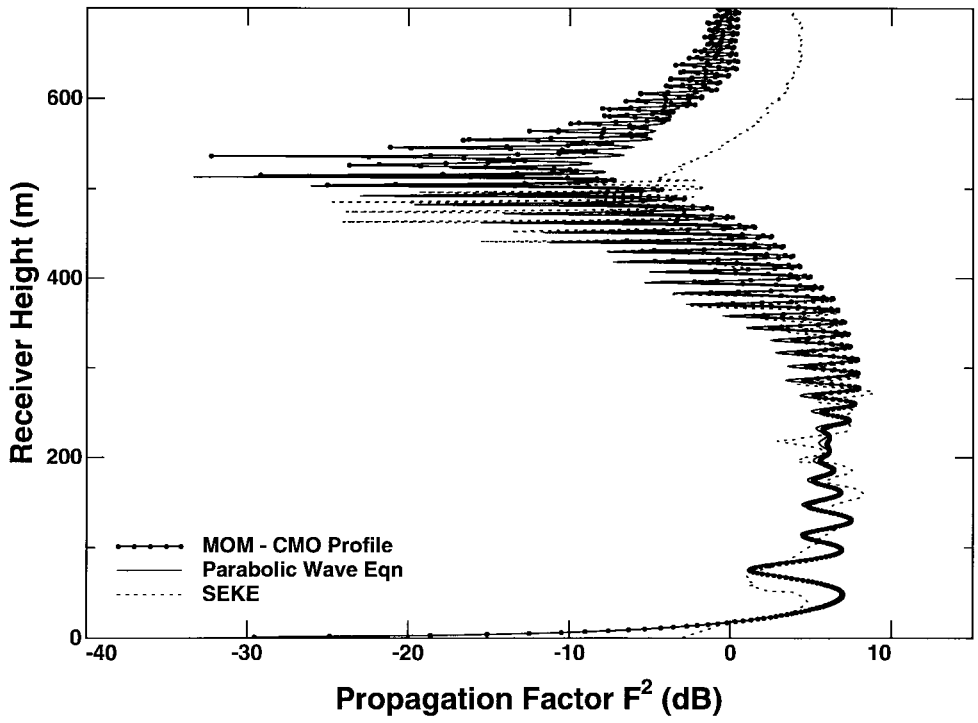

Fig. 9. Comparison with analytic models—Beiseker N15 CMO terrain profile.

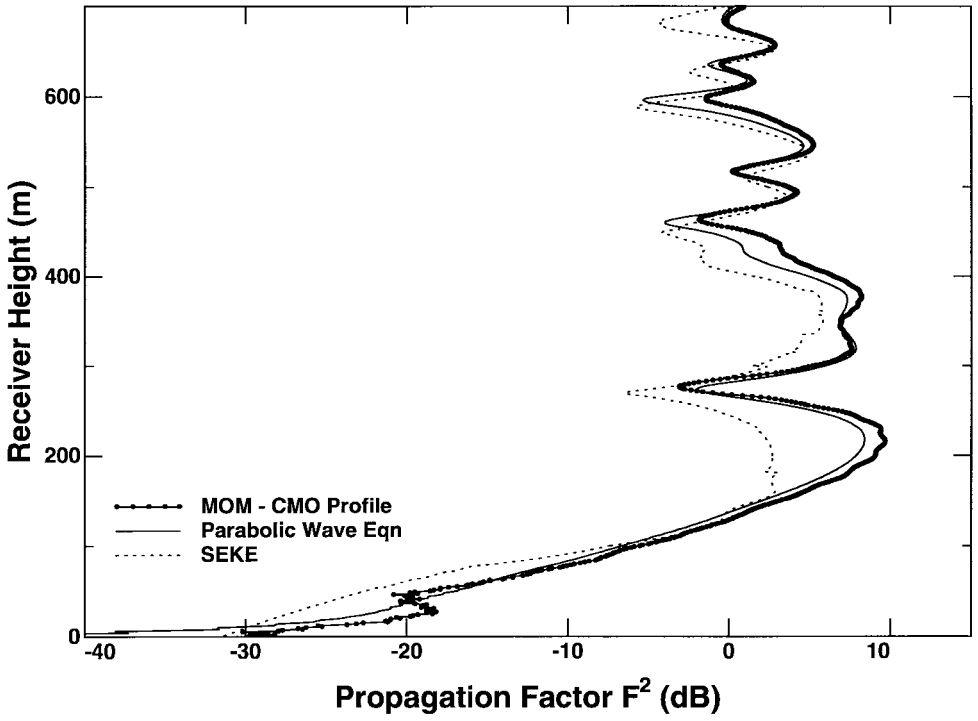

Fig. 10. Comparison with analytic models—Magrath NW27 CMO terrain profile.

tion routines in reference [19] when compared to wedge diffraction. Inaccuracies in SEKE's spherical and knife-edge diffraction weighting algorithm are seen in low-altitude regions (less than 20 m) as well, although improvements to SEKE for clutter modeling in this region have been studied and are currently being implemented [23]. SEKE also fails to obtain the small maximum at receiver height approximately 50 m in Figs. 10 and 11 which the PWE shows to be due to a bounce from a wave diffracted by the hill in the Magrath profile. Finally, the discrete nature of SEKE's routines is evident in Fig. 9, where the multiple specular contribution is included below receiver height 500 m, but abruptly ends above this height.

Agreement between PWE and MOM predictions is remarkable throughout Figs. 9–11, and illustrates the accuracy of the paraxial approximation for the terrain profiles investigated.

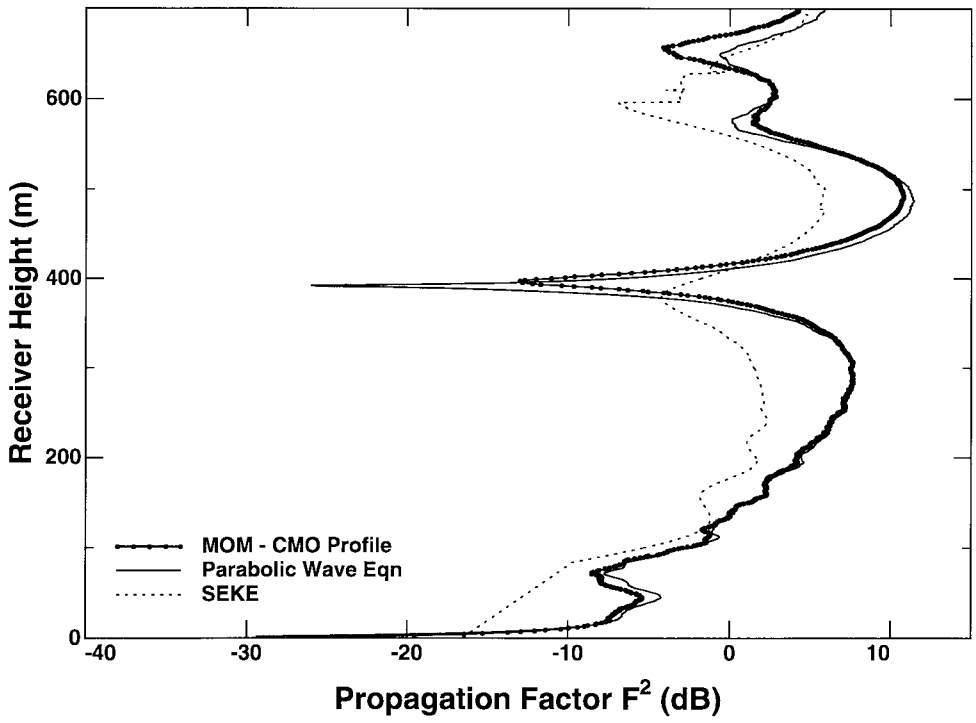

Fig. 11. Comparison with analytic models—Magrath NW37 CMO terrain profile.

Note that the criterion associated with selection of terrain profiles for the study was a failure of SEKE to match measurement data, so that no attempt was made to choose profiles which could cause PWE inaccuracies. The high accuracy of PWE results for these profiles, however, and their additional ability in modeling atmospheric structure clearly favors use of the PWE for propagation predictions. One disadvantage associated with the PWE is sensitivity to parameters used in the numerical simulation such as computational domain size, width of the initial field distribution, and properties of the upper absorbing boundary [5], [6]. For example, predictions generated for the Beiseker N15 profile of Fig. 9 were originally found inaccurate when a fairly narrow initial beam was used. Use of a wider initial-field distribution eliminated these problems, but caused errors due to spurious reflections from the 500-m fixed Gaussian taper computational domain upper boundary in longer range problems such as Magrath NW37. Although these errors were subsequently eliminated by doubling computational domain height from 8192 to 16 384 m for Magrath NW37, an appropriate choice of numerical simulation parameters is clearly required if reliable predictions are desired from the PWE. However, the relatively small amount of computational time required for the PWE makes an iterative procedure to determine simulation parameters feasible and the results of this study show that an iterated PWE technique should be a very accurate and practical tool for propagation prediction.

VII. Conclusions

A numerically exact model for VHF propagation based on an iterative version of the MOM has been developed. While this model remains computationally intense, its usefulness has been demonstrated in validating and studying the limitations of other approximate methods. Results have been shown which illustrate the accuracy of the numerical method and show the sensitivity of propagation models to input terrain profiles. Comparisons with the SEKE and PWE models showed that these models overall give reliable predictions, except in cases where underlying approximations become invalid. SEKE was found to follow the overall trends of the MOM in all cases, but to have problems in predicting propagation loss in regions where multiple phenomena were important. Agreement with the PWE was found to be excellent in all cases after steps were taken to insure that initial field distributions and computational domain sizes were appropriate.

Acknowledgment

The use of the IBM SP/2 at the Maui High Performance Computing Center was supported by the Phillips Laboratory, Air Force Material Command under cooperative agreement F29601-93-2-0001.

References

[1] S. Ayasli, "SEKE: A computer model for low altitude radar propagation over irregular terrain," *IEEE Trans. Antennas Propagat.*, vol. AP-34, pp. 1013–1023, Aug. 1986.
[2] S. T. McDaniel, "Propagation of a normal mode in the parabolic approximation," *J. Acoust. Soc. Amer.*, vol. 57, no. 2, pp. 307–311, 1975.
[3] G. D. Dockery, "Modeling electromagnetic wave propagation in the troposphere using the parabolic equation," *IEEE Trans. Antennas Propagat.*, vol. 36, pp. 1464–1470, 1988.
[4] J. R. Kuttler and G. D. Dockery, "Theoretical description of the parabolic approximation/Fourier split-step method of representing electromagnetic propagation in the troposphere," *Radio Sci.*, vol. 26, pp. 381–393, 1991.
[5] F. J. Ryan, "RPE: A parabolic equation radio assessment model," in *AGARD Conf. Proc. Operational Decision Aids Exploiting Mitigating Electromagn. Propagat. Effects*, 1989, pp. 19.1–19.10.

[6] ———, "Analysis of electromagnetic propagation over variable terrain using the parabolic wave equation," NOSC Tech. Rep. 1453, 1991.
[7] A. E. Barrios, "A terrain parabolic equation model for propagation in the troposphere," *IEEE Trans. Antennas Propagat.*, vol. 42, no. 1, pp. 90–98, 1994.
[8] M. F. Levy, "Horizontal parabolic equation solution of radiowave propagation problems on large domains," *IEEE Trans. Antennas Propagat.*, vol. 43, pp. 137–144, Feb. 1995.
[9] R. Janaswamy, "A fast finite difference method for propagation predictions over irregular, inhomogeneous terrain," *IEEE Trans. Antennas Propagat.*, vol. 42, pp. 1257–1267, Sept. 1994.
[10] ———, "A Fredholm integral equation method for propagation over small terrain irregularities," *IEEE Trans. Antennas Propagat.*, vol. 40, pp. 1416–1422, Nov. 1992.
[11] L. Tsang, C. H. Chan, K. Pak, H. Sangani, A. Ishimaru, and P. Phu, "Monte Carlo simulations of large scale composite random rough surface scattering based on the banded matrix iterative approach," *J. Opt. Soc. Amer.*, vol. 11, no. 2, pp. 691–696, 1994.
[12] C. H. Chan, L. Li, and L. Tsang, "A banded matrix iterative approach to Monte Carlo simulations of large scale random rough surface scattering: Penetrable case," in *9th Ann. Rev. Progress Appl. Computat. Electromagn. Conf. Proc.*, 1993, pp. 391–397.
[13] K. Pak, L. Tsang, C. H. Chan, and J. T. Johnson, "Backscattering enhancement of electromagnetic waves from two dimensional perfectly conducting random rough surfaces based on Monte Carlo simulations," *J. Opt. Soc. Amer. A*, vol. 12, no. 11, pp. 2491–2499, 1995.
[14] J. T. Johnson, L. Tsang, R. T. Shin, K. Pak, C. H. Chan, A. Ishimaru, and Y. Kuga, "Backscattering enhancement of electromagnetic waves from two dimensional perfectly conducting random rough surfaces: A comparison of Monte Carlo simulations with experimental data," *IEEE Trans. Antennas Propagat.*, vol. 44, pp. 778–756, May 1996.
[15] J. A. Kong, *Electromagnetic Wave Theory*, 2nd ed. New York: Wiley, 1990.
[16] J. R. Wait, *Electromagnetic Waves in Stratified Media*, 2nd ed. New York: Pergamon Press, 1970.
[17] R. F. Harrington, *Field Computation by Moment Methods*. New York: Macmillan, 1968.
[18] V. Liepa, "Numerical approach for predicting radiation patterns of HF-VHF antennas over irregular terrain," *IEEE Trans. Antennas Propagat.*, vol. AP-16, pp. 273–274, Mar. 1968.
[19] R. Luebbers, "Finite conductivity uniform GTD versus knife edge diffraction in prediction of propagation path loss," *IEEE Trans. Antennas Propagat.*, vol. AP-32, pp. 70–76, Jan. 1984.
[20] A. Geist, A. Beguelin, J. Dongarra, W. Jiang, R. Manchek, and V. Sunderam, "PVM 3 user's guide and reference manual," Oak Ridge National Laboratory Rep. ORNL/TM-12187, May 1994.
[21] W. L. Patterson, "Historical electromagnetic propagation condition database description," NOSC Tech. Doc. 1149, Sept. 1987.
[22] G. T. Huang and R. T. Shin, "Theoretical models for low-altitude propagation over terrain," in *Conf. Proc. Progress Electromagn. Res. Symp.*, 1993, p. 931.
[23] G. T. Huang, "Propagation over knife edge obstacles on a spherical earth," Dept. Elect. Eng. Comput. Sci., Massachusetts Inst. Technol., S.M. thesis, May 1992.

Joel T. Johnson (M'96) received the B.S. degree in electrical engineering from the Georgia Institute of Technology, Atlanta, in 1991, and the S.M. and Ph.D. degrees from the Massachusetts Institute of Technology, Cambridge, in 1993 and 1996, respectively.

He is currently an Assistant Professor in the Department of Electrical Engineering and ElectroScience Laboratory, The Ohio State University, Columbus. His research interests are in the areas of wave propagation, microwave remote sensing, and electromagnetic theory.

Dr. Johnson is a member of Tau Beta Pi, Eta Kappa Nu, and Phi Kappa Phi. He held a National Science Foundation graduate fellowship from 1991 to 1995 and received the 1993 Best Paper Award from the IEEE Geoscience and Remote Sensing Society.

Robert T. Shin (S'82–M'83–SM'90) received the B.S., M.S., and Ph.D. degrees all in electrical engineering from the Massachusetts Institute of Technology (MIT), Cambridge, in 1977, 1980, 1984, respectively.

Since 1984, he has been a member of MIT Lincoln Laboratory, as a Research Staff Member from 1984 to 1989, as a Senior Staff Member from 1989 to 1992, and as an Assistant Group Leader since 1992. Since 1987 he has served on the editorial board of the *Journal of Electromagnetic Waves and Applications* (JEWA). His research interests are in the areas of electromagnetic wave scattering and propagation, and theoretical model development and data interpretation for microwave remote sensing. He is a coauthor of *Theory of Microwave Remote Sensing* (New York: Wiley, 1985).

Dr. Shin is a member of the Electromagnetics Academy, Americal Geophysical Union, Tau Beta Pi, Eta Kappa Nu, and Commission F of the International Union of Radio Science.

John C. Eidson (M'92) received the B.S., M.S., and Ph.D. degrees in physics from the Georgia Institute of Technology, Atlanta, in 1984, 1985, and 1987, respectively, and the M.A. in biblical studies, in 1994, from the Dallas Theological Seminary, TX.

From 1987 to 1992, and since 1995, he has been a Technical Staff Member at the Massachusetts Institute of Technology (MIT) Lincoln Laboratory, Cambridge, MA. His current research interests are in the areas of electromagnetic propagation, radar ground clutter, and radar system performance.

Leung Tsang (S'73–M'75–SM'85–F'90) received the S.B., S.M., and Ph.D. degrees from Massachusetts Institute of Technology (MIT), Cambridge, in 1971, 1973, and 1976, respectively.

He has been a Professor of electrical engineering at the University of Washington, Seattle, since 1986. He is a co-author of *Theory of Microwave Remote Sensing* (New York: Wiley, 1985). Since 1996, he has been the Editor of the IEEE TRANSACTIONS ON GEOSCIENCE AND REMOTE SENSING. His current research interests are in remote sensing, wave propagation in random media and rough surfaces, and optoelectronics.

Dr. Tsang is a Fellow of the Optical Society of America. He was the Technical Program Chairman of the 1994 IEEE Antennas and Propagation International Symposium and was also the Technical Program Chairman of the 1995 Progress in Electromagnetics Research Symposium.

Jin Au Kong (S'65–M'69–SM'74–F'85) is a Professor of electrical engineering at the Massachusetts Institute of Technology (MIT), Cambridge. He has published eight books including *Electromagnetic Wave Theory* (New York: Wiley, 1990), more than 400 refereed articles and book chapters, and supervised more than 120 theses. He is Editor-in-Chief of the *Journal of Electromagnetic Waves and Applications*, chief editor of the book series *Progress in Electromagnetics Research*, and editor of the *Wiley Series in Remote Sensing*. His research interest is in the area of electromagnetic wave theory and applications.